Voxel-Based and Surface-Based Morphometry Study of the Early Stage of Carbon Monoxide Poisoning-Induced Parkinsonism

Tianhong Wang
Lanzhou University First Affiliated Hospital
Yanli Zhang
Lanzhou University First Affiliated Hospital
Junxia Xu
Lanzhou University First Affiliated Hospital
Junqiang Lei
Lanzhou University First Affiliated Hospital
Shunlin Guo (guo_ky2021@163.com)
Lanzhou University First Affiliated Hospital https://orcid.org/0000-0002-7803-7861

Research Article

Keywords: carbon monoxide poisoning, parkinsonism, structural MRI, morphological analysis, motor disorder

Posted Date: July 12th, 2022

DOI: https://doi.org/10.21203/rs.3.rs-1777825/v1

Abstract

Grey matter (GM) volume changes in carbon monoxide poisoning (COP)-induced parkinsonism have been investigated in previous studies. However, a combined analysis of GM and white matter (WM) volume, cortical thickness, and shape is lacking. Eighteen COP-induced parkinsonism patients and 22 matched healthy controls (HCs) were enrolled in this study. All MRI scans were performed within 3 months after COP and analysed with a combination of voxel- and surface-based morphometry (VBM and SBM) analyses. Relationships between structural changes and clinical scores were detected with partial correlation analysis. VBM analysis showed reduced GM volumes in the bilateral frontal and temporal lobes, anterior cingulate cortex (ACC), amygdala, striatum, thalamus, and cerebellum (FDR-corrected $P < 0.001$) and a trend towards WM atrophy in the anterior cerebral and medial mesencephalon but swelling in the posterior cerebral and motor cortical areas (uncorrected $P < 0.001$) in the patients. SBM analysis showed widespread cortical thinning that extended beyond the frontotemporal regions and involved the occipitoparietal areas and regional shallow sulcal depth in the left supramarginal gyrus in the patients (FWE-corrected $P < 0.05$). The severity of motor disorders was correlated with GM atrophy in the medial orbital superior frontal gyrus (SFG), ACC, caudate, thalamus, and caudal middle frontal gyrus, while nonmotor disorders were correlated with atrophy in the SFG, ACC, thalamus, amygdala, and cerebellum crus I (all $P < 0.05$). Early-stage COP-induced parkinsonism is characterised by widespread GM atrophy. A combination of VBM and SBM analyses contributes to revealing its imaging pathological feature.

Introduction

Parkinsonism following carbon monoxide poisoning (COP) is a well-known syndrome that occurs in approximately 10% of patients and usually develops within 1 month after a latency period that varies from 2 to 26 (median 4) weeks (Choi, 2002). Unlike the less cognitive and more profound behavioural changes that appear early in Parkinson's disease (PD), patients with COP-induced parkinsonism often present with urinary and faecal incontinence, cognitive deficits, and/or psychiatric behavioural abnormalities in the early stage (Choi, 2002; Kao, et al., 2012). Tremors are rarely observed in COP-induced parkinsonism, and treatments with levodopa and anticholinergic drugs are usually less effective in these patients (Choi, 2002; Chang,et al., 2015). From the view of the specific pathologies, it has been suggested that the lateral and middle segments of the substantia nigra are more susceptible to COP-induced parkinsonism than the lateral and medial segments that are affected in PD (Kao, et al.,2012; Ma,et al.,1996).

Previous studies have detected pathological imaging changes in COP-induced parkinsonism in the extranigral regions. A study revealed monoaminergic deficits in networks with chronic-stage COP-induced parkinsonism that consist of the caudate, anterior putamen, anterior insula, thalamus and anterior cingulate cortex (ACC), and this distribution overlapped with the regions showing reduced grey matter (GM) volume (Chang, et al., 2015). Another study showed alterations in glucose metabolism in networks consisting of the frontotemporoparietal cortices and striatum and GM atrophy in networks consisting of the prefrontal and lateral temporal cortices, caudate, and thalamus in COP-induced parkinsonism at 4.8 ±

0.8 months after COP (Chang, et al., 2016). Clearly, these studies have revealed a much deeper involvement of the GM and cerebral cortex in the neuronal networks affected by COP-induced parkinsonism that is accompanied by functional and structural changes both in the early and chronic stages.

In addition to GM injuries, greater white matter (WM) lesions and lower fractional anisotropy (FA) values in WM tissue were suggested to be associated with COP-induced parkinsonism (Sohn, et al., 2000;Chou, et al., 2019). A previous study further demonstrated that early COP-induced WM injuries in dopaminergic pathways led to dopamine transporter (DAT) dysfunction in the striatum and parkinsonism symptoms observed in COP patients (Chang,et al., 2011). However, the whole-brain WM atrophy pattern involved in COP-induced parkinsonism is still uncertain.

As a commonly used structural analysis method, voxel-based morphometry (VBM) identifies regional GM and WM volume changes in the whole brain. Surface-based morphometry (SBM), a well-validated and highly accurate method, allows the analysis of additional cortical morphological features using multiple parameters, including cortical thickness and shape (gyrification, sulcal depth, and fractal dimension). Previous studies have discussed patterns of PD-related cortical morphological changes that include cortical thinning (Menke, et al., 2014; Jubault, et al., 2011; Filippi, et al., 2020; Gao, et al., 2020; Zarei, et al., 2011; Zhang, et al., 2014) or gyrification reductions (Zhang,et al., 2014) in multiple brain regions. It was also shown that SBM analyses were more sensitive than VBM analyses for detecting cortical changes in the group comparison (Menke, et al., 2014). However, to our knowledge, no study has investigated these cortical morphometric patterns in patients with COP-induced parkinsonism using SBM analysis.

Therefore, in the current study, we aimed to conduct a comprehensive analysis of GM and WM volume, cortical thickness, and shape in a group of early-stage COP-induced parkinsonism patients using two different morphometric analyses (VBM and SBM). Additionally, we investigated the correlations between abnormal brain structure and motor disorders, cognitive impairments, and neuropsychiatric severity.

Materials And Methods

Patient Enrolment

The Department of Neurology of the First Hospital of Lanzhou University recruited COP-induced parkinsonism patients from October 2018 to January 2022. These patients satisfied the following inclusion criteria: 1) a clear history of recent CO exposure within three months; 2) at least two of the following symptoms occurring in a progressive or delayed relapsing course after COP: hypokinesia, rigidity, tremor, gait disturbances and postural instability; 3) all patients were right-handed. Faulty stoves and inadequate ventilation of heating sources can result in the release of CO-containing gas into living spaces from heating charcoal stoves, which are the main heating systems used in households in winter in the northwest region of China.

Patients were excluded if they had any evidence of 1) being younger than 18 years old or older than 70 years; 2) evidence of brain disorders, including traumatic brain injury, neuropsychiatric disorders, operation, stroke, infection, neoplasm, and demyelinating diseases; or 3) being unable to complete the neurologic functional evaluation within 24 h after the MRI scan.

The neurological assessments were administered after MRI scans on the same day. The severity of parkinsonism was evaluated using the Unified Parkinson's Disease Rating Scale subsection III (UPDRS III) motor score. General cognition was assessed using the Mini-Mental State Examination (MMSE) and Montreal Cognitive Assessment (MoCA) tests. The Neuropsychiatric Inventory (NPI) was used to assess psychiatric and behavioural disorders.

In addition, 22 sex-, age-, and education-matched healthy subjects were enrolled as healthy controls (HCs). The ethics committee of The First Hospital of Lanzhou University approved the study (LDYYLL2018-114). Informed consent was obtained from each participant.

MRI Acquisition

All images were acquired on a 3T MR imaging system (Magneton Skyra; Siemens, Erlangen, Germany) with a 32-channel phased-array head coil. After conventional T2WI, T2 FLAIR and DWI scans, whole-brain high-resolution T1WI data were acquired using a magnetization-prepared rapid acquisition gradient echo sequence with the following parameters: repetition (TR), echo (TE) and inversion (TI) times = 2300/2.98/900 ms, respectively; flip angle = 9 degrees; matrix size = 256 × 256 mm; slice thickness = 1 mm; and number of slices = 176. All scans were performed by the same technician using the same positioning baseline and parameters.

MRI Data Preprocessing

The VBM and SBM analyses were executed using the CAT12 toolbox (http://www.neuro.uni-jena.de/cat/) building on the Statistical Parametric Mapping 12 toolbox (http://www.fil.ion.ucl.ac.uk/spm/software/spm12/), running on the MATLAB 2016a platform. Default parameters in accordance with the standard protocol were used in segmentation, surface estimation, data resampling, and smoothing.

For VBM analyses, images were segmented into GM, WM, and cerebrospinal fluid and spatially normalised with the DARTEL algorithm. Images were smoothed with a Gaussian kernel of 10 mm [full width at half maximum (FWHM)]. The total intracranial volume (TIV) was determined as the sum of the GM, WM and cerebrospinal fluid volumes.

We extracted SBM parameters, including cortical thickness, gyrification, sulcal depth, and fractal dimension. As recommended, the smoothing filter size in FWHM was 15 mm for the thickness data and 20 mm for the folding data (gyrification, sulcal depth, and fractal dimension). All of the preprocessed data were visually inspected for artefacts and homogeneity, and the overall image quality was checked for statistical quality control.

Statistical Analyses

The data are presented as the means ± standard deviations. Two independent-sample *t* tests or Mann–Whitney *U* tests were performed to assess the differences in age, education, VBM and SBM metrics, and neurological assessment scores, and the chi-square test was used to compare the sex composition of the two groups using the Statistical Package for Social Sciences software package (Version 22 for Windows; IBM, Armonk, New York). The threshold for statistical significance was a *P* value < 0.05.

Two independent-sample *t* tests were performed with the covariates age and sex to investigate regional differences in GM and WM volume, cortical thickness, gyrification, sulcal depth, and fractal dimension using SPM12. In the VBM analyses, TIV was included as an additional covariate. In view of the claim that a more stringent *P* value threshold could also lead to more false negatives as emphasized in a recent study (Jia,et al., 2021), we made adjustments using different correction methods [familywise error (FWE) or false discovery rate (FDR)] to identify the potential differences after an initial voxel- or vertex-level uncorrected threshold of *P* < 0.001. Partial correlation analyses adjusted for age, sex, and education were performed to assess the correlation between clinical scores and the volume, thickness and shape characteristics in each significant cluster using SPSS 22. The threshold for statistical significance was a *P* value < 0.05.

Results

Patient Enrolment

The Department of Neurology of the First Hospital of Lanzhou University recruited COP-induced parkinsonism patients from October 2018 to January 2022. These patients satisfied the following inclusion criteria: 1) a clear history of recent CO exposure within three months; 2) at least two of the following symptoms occurring in a progressive or delayed relapsing course after COP: hypokinesia, rigidity, tremor, gait disturbances and postural instability; 3) all patients were right-handed. Faulty stoves and inadequate ventilation of heating sources can result in the release of CO-containing gas into living spaces from heating charcoal stoves, which are the main heating systems used in households in winter in the northwest region of China.

Patients were excluded if they had any evidence of 1) being younger than 18 years old or older than 70 years; 2) evidence of brain disorders, including traumatic brain injury, neuropsychiatric disorders, operation, stroke, infection, neoplasm, and demyelinating diseases; or 3) being unable to complete the neurologic functional evaluation within 24 h after the MRI scan.

The neurological assessments were administered after MRI scans on the same day. The severity of parkinsonism was evaluated using the Unified Parkinson's Disease Rating Scale subsection III (UPDRS III) motor score. General cognition was assessed using the Mini-Mental State Examination (MMSE) and Montreal Cognitive Assessment (MoCA) tests. The Neuropsychiatric Inventory (NPI) was used to assess psychiatric and behavioural disorders.

In addition, 22 sex-, age-, and education-matched healthy subjects were enrolled as healthy controls (HCs). The ethics committee of The First Hospital of Lanzhou University approved the study (LDYYLL2018-114). Informed consent was obtained from each participant.

MRI Acquisition

All images were acquired on a 3T MR imaging system (Magneton Skyra; Siemens, Erlangen, Germany) with a 32-channel phased-array head coil. After conventional T2WI, T2 FLAIR and DWI scans, whole-brain high-resolution T1WI data were acquired using a magnetization-prepared rapid acquisition gradient echo sequence with the following parameters: repetition (TR), echo (TE) and inversion (TI) times = 2300/2.98/900 ms, respectively; flip angle = 9 degrees; matrix size = 256 × 256 mm; slice thickness =1 mm; and number of slices = 176. All scans were performed by the same technician using the same positioning baseline and parameters.

MRI Data Preprocessing

The VBM and SBM analyses were executed using the CAT12 toolbox (http://www.neuro.uni-jena.de/cat/) building on the Statistical Parametric Mapping 12 toolbox (http://www.fil.ion.ucl.ac.uk/spm/software/spm12/), running on the MATLAB 2016a platform. Default parameters in accordance with the standard protocol were used in segmentation, surface estimation, data resampling, and smoothing.

For VBM analyses, images were segmented into GM, WM, and cerebrospinal fluid and spatially normalised with the DARTEL algorithm. Images were smoothed with a Gaussian kernel of 10 mm [full width at half maximum (FWHM)]. The total intracranial volume (TIV) was determined as the sum of the GM, WM and cerebrospinal fluid volumes.

We extracted SBM parameters, including cortical thickness, gyrification, sulcal depth, and fractal dimension. As recommended, the smoothing filter size in FWHM was 15 mm for the thickness data and 20 mm for the folding data (gyrification, sulcal depth, and fractal dimension). All of the preprocessed data were visually inspected for artefacts and homogeneity, and the overall image quality was checked for statistical quality control.

Statistical Analyses

The data are presented as the means ± standard deviations. Two independent-sample *t* tests or Mann–Whitney *U* tests were performed to assess the differences in age, education, VBM and SBM metrics, and neurological assessment scores, and the chi-square test was used to compare the sex composition of the two groups using the Statistical Package for Social Sciences software package (Version 22 for Windows; IBM, Armonk, New York). The threshold for statistical significance was a P value < 0.05.

Two independent-sample *t* tests were performed with the covariates age and sex to investigate regional differences in GM and WM volume, cortical thickness, gyrification, sulcal depth, and fractal dimension

using SPM12. In the VBM analyses, TIV was included as an additional covariate. In view of the claim that a more stringent *P* value threshold could also lead to more false negatives as emphasized in a recent study (Jia,et al., 2021), we made adjustments using different correction methods [familywise error (FWE) or false discovery rate (FDR)] to identify the potential differences after an initial voxel- or vertex-level uncorrected threshold of $P < 0.001$. Partial correlation analyses adjusted for age, sex, and education were performed to assess the correlation between clinical scores and the volume, thickness and shape characteristics in each significant cluster using SPSS 22. The threshold for statistical significance was a *P* value < 0.05.

Discussion

In the current study, we first investigated patterns of GM and WM volume changes between groups using whole-brain VBM and compared cortical thickness and shape using whole-brain SBM in the same groups. The VBM analysis allows us to compare our results with previous VBM studies. The SBM analysis provided additional cortical morphologic metrics. Different patterns of morphological changes, highlighting specific disease trajectories, could potentially generate neuroimaging-derived biomarkers and help us to understand the neural mechanisms underlying early-stage COP-induced parkinsonism. Furthermore, we determined how neurological disorders of the COP-induced parkinsonism are associated with our neuroanatomical findings.

We found significantly reduced GM volume in several regions, including the bilateral medial prefrontal cortices, temporal lobes, ACC, amygdala, olfactory bulb, caudate, putamen, thalamus, and cerebellum, in the patients 3 months after COP. Chang et al reported that, with an FDR-corrected $P < 0.01$ and an extended threshold of 250 voxels, regions showing greater GM atrophy in early-stage COP-induced parkinsonism patients (the mean interval from CO intoxication to the study was 4.8 ± 0.8 months) were located in the medial and lateral prefrontal cortices, lateral temporal cortex, caudate, and thalamus (Chang, et al., 2016). A previous study reported that in chronic patients (an average interval period from CO poisoning of 19.38 months) significant atrophy was observed in regions including the caudate, anterior putamen, anterior insula, thalamus, ACC, and dorsolateral prefrontal cortex (cluster–enhancement-corrected $P < 0.05$) (Chang,et al.,2015). In our study, in addition to the common regions showing atrophy, including the frontotemporal areas, ACC, striatum, and thalamus, we found atrophy in regions including the amygdala, olfactory bulb, and CERCRU I and VI. Moreover, there was a significant negative correlation between atrophy in the amygdala and the NPI scores and a positive correlation between atrophy in the CERCRU I and the MMSE and MoCA scores (all $P < 0.05$). The amygdala has long been associated with emotion and motivation and plays an essential part in processing both affect and cognition. Motor representation in the cerebellar anterior lobe (and adjacent region of lobule VI) and nonmotor representation in the cerebellar posterior lobe in lobule VI, crus I and II have been reported in task-based and resting-state functional MRI in humans (Schmahmann,et al., 2019).There were no significant correlations between atrophy in the amygdala, olfactory bulb, and CERCRU I and VI and UPDRS III scores. A previous study showed that MMSE and NPI scores could predict the presence or absence of parkinsonism in patients with COP (Sun, et al., 2018). Therefore, we speculated that these

areas might indirectly take mediate the motor disorder by directly influencing cognitive and emotional processing.

Of note, our VBM analysis showed that the left caudate and putamen had a tendency to show more atrophy than the right caudate and putamen; moreover, left caudate imaging metrics were related to the severity of motor disorders (r = -0.547, P = 0.035). Asymmetrical striatal DAT binding in healthy subjects has been reported, with higher binding rates on the left side than on the right side (Van Dyck, et al., 2002). Lower binding of the left striatal DAT could help to predict the development of delayed neuropsychological sequelae after CO poisoning (Yang, et al., 2011) .Their findings provide a basic theory to help us understand the asymmetrical caudate and putamen atrophy observed in our patients. In addition to the above brain regions, we found that atrophy in the bilateral thalamus, ACC and medial orbital SFG was significantly correlated with parkinsonism severity and cognitive and psychiatric behavioural disorders (all P< 0.05). This is coincident with a previous multimodal imaging study, which reported that the regions that jointly explained the parkinsonian and cognitive features included the thalamus, caudate, ACC, and SFG regions in early-stage COP-induced parkinsonism (Chang, et al., 2015).

Additionally, symmetrical hyperintensity on T2WI of the globus pallidus was the only visual GM injury in our patients. Meanwhile, dopaminergic neuronal loss in the substantia nigra is a prototypical feature of PD. However, it was seemingly counterintuitive that we did not find atrophy in these two important areas. A better designed study is necessary to further explore the underlying pathological mechanisms.

Importantly, although we did not detect any WM volume change with strict correction of multiple comparisons, we found a trend of reduced WM volume in the anterior corona radiata, prefrontal periventricular regions, and medial mesencephalon and increased WM volume in the bilateral precentral and postcentral gyri, left thalamus, bilateral optic radiation and occipital lobe in our patients (uncorrected P< 0.001). This hinted at underlying pathological changes: the atrophy of the WM in the anterior cerebral and medial mesencephalon was accompanied by swelling of WM in the posterior cerebral and motor areas, suggesting earlier damage to the anterior WM. Importantly, the pattern of atrophy in anterior WM overlapped the decreased volume and thickness in the prefrontal cortex. Chang et al (Chang, et al., 2011) reported that WM integrity changes in the mesencephalic-basal ganglia-cortical network might be related to COP-induced parkinsonism. They found that the rostral fibre projections from the mesencephalon substantia nigra course through the globus pallidus and that the frontal periventricular region terminates bilaterally in the supplementary motor area and the ACC (Chang, et al., 2011). Similarly, by combining the volume and thickness analysis, we found that WM atrophy in the mesencephalon-periventricular regions-anterior corona radiata correspond to GM atrophy in the basal ganglia and the anterior cingulate, prefrontal, and motor cortices. This could be explained by the fact that WM fibres in the mesencephalon and prefrontal regions affect substantia nigra dopaminergic projection sites (putamen and caudate nucleus) and lead to ineffective connections between the prefrontal and motor cortices, resulting in their most overlapping patterns of atrophy.

We found no significant regional gyrification and fractal dimension differences between the groups; meanwhile, only reduced sulcal depth in the left supramarginal gyrus appeared in the patient group. However, thickness analysis showed widespread cortical thinning in the bilateral motor cortices, lateral and medial prefrontal cortices, dorsolateral temporal region, and occipital and parietal lobes. It was affirmed that thickness measurements are more sensitive than shape and volume measurements to differentiate subtle cortical changes. This is consistent with a previous PD study. Kunst et al (Kunst, et al., 2019) reported that only thickness measurements revealed differences between PD patients with normal cognition and HCs when comparing the volume, thickness and shape indices in the same group of patients. Furthermore, we found that cortical thinning extended beyond anterior regions (reduced GM volume in frontal and temporal) and involved posterior areas (occipital and parietal lobes). Early-stage posterior cortical thinning has been recently demonstrated in PD patients in association with reduced striatal DAT uptake (Winkler,et al., 2010). Moreover, posterior cortical thinning in PD is currently known to play a major role in the development of PD dementia (Sampedro, et al., 2019). Certainly, there was no significant correlation between posterior cortical thinning and cognitive and motor scores in the current results, suggesting a minor contribution to abnormal neurological function. A longitudinal study might be helpful to explore the underlying pathological significance related to cortical thinning in the occipital and parietal lobes. Correlation analysis further showed that cortical thinning in the bilateral caudal MFG (belonging to the premotor area) was negatively correlated with UPDRS III scores ($P < 0.05$), suggesting that the thinning premotor area cortex contributed to parkinsonian severity. There was also a significant positive correlation between cortical thinning in the bilateral SFG and MoCA scores ($P < 0.05$). This again emphasized the role of the SFG in mediating cognitive disorders, as shown by the VBM analysis.

Local folding has been suggested to reflect the state of the underlying WM fibres (Filippi, et al., 2020), as more tension or shrinkage of these fibres could lead to deeper sulc (Van Essen, et al., 1997). We found a trend towards shallow sulcal depth mostly involved in the parietal and occipital lobes and supplementary motor area (uncorrected $P < 0.001$), which partly overlapped the regions with WM swelling. We inferred that the increased WM volume gave rise to the expanding cortex and shallower sulcal depth. Certainly, the proposed mechanisms are purely speculative and have to be exclusively considered alternative explanations.

Limitations

There are some limitations to our study. First, as a cross-sectional study with a small number of subjects, a large sample size and longitudinal follow-up study is necessary to explain dynamic changes in GM and WM volume and cortical morphology with changes in disease duration. Second, all patients in this study were treated with hyperbaric oxygen and drugs, and we cannot rule out the possible effect of treatment in the volume and shape analyses. Third, in the early stage, patients with COP-induced parkinsonism usually have nonmotor symptoms, such as cognitive impairment, depression, anxiety, and apathy. It would be difficult to add new subgroups with different nonmotor symptoms to reveal more special symptom-related structural alterations.

Conclusions

In summary, widespread abnormalities in GM volume, cortical thickness and regional sulcal depth were characteristic of patients with early-stage COP-induced parkinsonism. Among these, the atrophy in the medial prefrontal cortex, premotor cortex, ACC, caudal regions, and thalamus mainly contributed to parkinsonism severity. These findings across different imaging analyses supply complementary information and reveal the specific pathological characteristics in this disorder. Indeed, structural MRI is a less invasive and costly technique, and this approach could become clinically relevant if it can be developed to become sensitive enough at the single-patient level.

Abbreviations

SFG, superior frontal gyrus; MFG, middle frontal gyrus; ACC, anterior cingulate cortex; MTG, middle temporal gyrus; ITG, inferior temporal gyrus; CERCRU I, cerebellum crus I; CERCRU VI, cerebellum lobule VI; SPG, superior parietal gyrus; IPG, inferior parietal gyrus; LOL, lateral occipital lobes.

Declarations

Ethics approval The study protocol was approved by the the ethics committee of The First Hospital of Lanzhou University.

Consent to participate The written informed consent form was obtained from all subjects prior to their participation.

Consent to publication The manuscript is approved by authors for publication.

Author contributions Tianhong Wang and Yanli Zhang contributed equally to this work.Tianhong Wang collected MRI and clinical data, performed analysis and wrote the manuscript.Yanli Zhang contributed to the data analysis and interpretation. Junxia Xu helped with data collection. Junqiang Lei participated in the design of the study and provided the main idea for the manuscript. Shunlin Guo designed the experiments and contributed to the manuscript revision.

Funding This study was supported by research grants from the national natural science foundation of china (Grant number: 82160930) and the research project of gansu provincial administration of traditional chinese medicine (Grant number: GZKZ-2021-8)

Competing Interests The authors declare that they have no conflict of interest.

Availability of data and materials All data during the study appear in the submitted article and are available from the corresponding author upon reasonable request.

References

1. Chang, C. C., Chang, W. N., Lui, C. C., Huang, S. H., Lee, C. C., Chen, C., Wang, J. J. (2011). Clinical significance of the pallidoreticular pathway in patients with carbon monoxide intoxication. *Brain* ,134, 3632–3646.
2. Chang, C. C., Hsiao, I. T., Huang, S. H., Lui, C. C., Yen, T. C., Chang, W. N., Huang, C. W., Hsieh, C. J., Chang, Y. Y., Lin, K. J. (2015). ¹⁸F-FP-(+)-DTBZ positron emission tomography detection of monoaminergic deficient network in patients with carbon monoxide related parkinsonism. *Eur.J. Neurol*, 22, 845–e60.
3. Chang, C. C., Hsu, J. L., Chang, W. N., Huang, S. H., Huang, C. W., Chang, Y. T., Chen, N. C., Lui, C. C., Lee, C. C., Hsu, S. W. (2016). Metabolic Covariant Network in Relation to Nigrostriatal Degeneration in Carbon Monoxide Intoxication-Related Parkinsonism. *Front. Neurosci*, 10,187.
4. Choi I.S. (2002). Parkinsonism after carbon monoxide poisoning. *Eur Neurol*, 48, 30–33.
5. Chou, M. C., Lai, P. H., Li, J. Y. (2019). Early white matter injuries associated with dopamine transporter dysfunction in patients with acute CO intoxication: A diffusion kurtosis imaging and Tc-99m TRODAT-1 SPECT study. *Eur Radiol*, 29, 1375–1383.
6. Filippi, M., Canu, E., Donzuso, G., Stojkovic, T., Basaia, S., Stankovic, I., Tomic, A., Markovic, V., Petrovic, I., Stefanova, E., Kostic, V. S., Agosta, F. (2020). Tracking Cortical Changes Throughout Cognitive Decline in Parkinson's Disease. *Mov Disord*, 35, 1987–1998.
7. Gao, Y., Nie, K., Mei, M., Guo, M., Huang, Z., Wang, L., Zhao, J., Huang, B., Zhang, Y., Wang, L. (2018). Changes in Cortical Thickness in Patients With Early Parkinson's Disease at Different Hoehn and Yahr Stages. *Front Hum Neurosci*, 12, 469.
8. Jia, Xi-Ze.,Zhao, Na.,Dong, Hao-Ming.,Sun, Jia-Wei.,Barton, Marek., Burciu, Roxana.,Carriere, Nicolas.,Cerasa, Antonio.,Chen, Bo-Yu., Chen, Jun. (2021).Small P values may not yield robust findings: an example using REST-meta-PD.*Science Bulletin*, 66,2148-2152.
9. Jubault, T., Gagnon, J. F., Karama, S., Ptito, A., Lafontaine, A. L., Evans, A. C., Monchi, O. (2011). Patterns of cortical thickness and surface area in early Parkinson's disease. *Neuroimage*, 55, 462–467.
10. Kao, H. W., Cho, N. Y., Hsueh, C. J., Chou, M. C., Chung, H. W., Liou, M., Chiang, S. W., Chen, S. Y., Juan, C. J., Huang, G. S., Chen, C. Y. (2012). Delayed parkinsonism after CO intoxication: evaluation of the substantia nigra with inversion-recovery MR imaging. *Radiology*, 265, 215–221.
11. Kunst, J., Marecek, R., Klobusiakova, P., Balazova, Z., Anderkova, L., Nemcova-Elfmarkova, N., Rektorova, I. (2019). Patterns of Grey Matter Atrophy at Different Stages of Parkinson's and Alzheimer's Diseases and Relation to Cognition. *Brain Topogr*, 32, 142–160.
12. Ma, S. Y., Rinne, J. O., Collan, Y., Röyttä, M., Rinne, U. K. (1996). A quantitative morphometrical study of neuron degeneration in the substantia nigra in Parkinson's disease. *J.Neurol Sci*, 140, 40–45.
13. Menke, R. A., Szewczyk-Krolikowski, K., Jbabdi, S., Jenkinson, M., Talbot, K., Mackay, C. E., Hu, M. (2014). Comprehensive morphometry of subcortical grey matter structures in early-stage Parkinson's

disease. *Hum Brain Mapp*, 35, 1681–1690.

14. Sampedro, F., Marín-Lahoz, J., Martínez-Horta, S., Pagonabarraga, J., Kulisevsky, J. (2019). Dopaminergic degeneration induces early posterior cortical thinning in Parkinson's disease. *Neurobiol Dis*, 124, 29–35.
15. Schmahmann, J. D., Guell, X., Stoodley, C. J.,Halko, M. A. (2019). The Theory and Neuroscience of Cerebellar Cognition. *Annu. Rev. Neurosci*, 42, 337–364.
16. Sohn, Y. H., Jeong, Y., Kim, H. S., Im, J. H., Kim, J. S. (2000). The brain lesion responsible for parkinsonism after carbon monoxide poisoning. *Arch Neurol*, 57, 1214–1218. .
17. Sun, T. K., Chen, Y. Y., Huang, S. H., Hsu, S. W., Lee, C. C., Chang, W. N., Huang, C. W., Lui, C. C., Lien, C. Y., Cheng, J. L., Chang, C. C. (2018). Neurotoxicity of carbon monoxide targets caudate-mediated dopaminergic system. *Neurotoxicology*, 65, 272–279.
18. Van Dyck, C. H., Seibyl, J. P., Malison, R. T., Laruelle, M., Zoghbi, S. S., Baldwin, R. M., Innis, R. B. (2002). Age-related decline in dopamine transporters: analysis of striatal subregions, nonlinear effects, and hemispheric asymmetries. Am. J .Geriatr .*Psychiatry* , 10, 36–43.
19. Van Essen D. C. (1997). A tension-based theory of morphogenesis and compact wiring in the central nervous system. Nature, 385, 313–318.
20. Winkler, A. M., Kochunov, P., Blangero, J., Almasy, L., Zilles, K., Fox, P. T., Duggirala, R., Glahn, D. C. (2010). Cortical thickness or grey matter volume? The importance of selecting the phenotype for imaging genetics studies. Neuroimage, 53, 1135–1146.
21. Yang, K. C., Ku, H. L., Wu, C. L., Wang, S. J., Yang, C. C., Deng, J. F., Lee, M. B., Chou, Y. H. (2011). Striatal dopamine transporter binding for predicting the development of delayed neuropsychological sequelae in suicide attempters by carbon monoxide poisoning: A SPECT study. Psychiatry Res, 194, 219–223.
22. Zarei, M., Ibarretxe-Bilbao, N., Compta, Y., Hough, M., Junque, C., Bargallo, N., Tolosa, E., Martí, M. J. (2013). Cortical thinning is associated with disease
23. stages and dementia in Parkinson's disease. J.Neurol Neurosurg Psychiatry, 84, 875–881.
24. Zhang, Y., Zhang, J., Xu, J., Wu, X., Zhang, Y., Feng, H., Wang, J., Jiang, T. (2014). Cortical gyrification reductions and subcortical atrophy in Parkinson's disease. Mov Disord, 29, 122–126.

Tables

Table 1
Demographic and clinical characteristics of COP-induced parkinsonism patients and HCs

	Healthy controls group (n = 22)	COP-induced parkinsonism Group(n = 18)	*P* value
Age, year (rang)	54.95 ± 5.72(49, 65)	55.50 ± 6.35(42, 69)	0.854
Sex (female/ male)	11/11	8/10	0.726
Education (years)	7.27 ± 4.10	7.00 ± 4.07	0.966
From COP to MRI scan (days)	-	59.06 ± 26.39	-
Gray matter volume (cm3)	611.53 ± 54.74	572.15 ± 80.08	0.073
White matter volume (cm3)	487.14 ± 47.22	533.64 ± 76.19	0.023 *
Total intracranial volume(cm3)	1364.22 ± 110.53	1455.00 ± 192.28	0.069
Thickness	2.69 ± 0.12	2.39 ± 0.19	0.000 *
Sulcal depth	519.18 ± 67.12	578.95 ± 41.42	0.001 *
Gyrification	1474.32 ± 25.91	1892.68 ± 41.92	0.000 *
Fractal dimension	151.29 ± 1.68	176.95 ± 3.38	0.000 *
MMSE	29.68 ± 0.57	21.72 ± 5.12	0.000 *
UPDRS motor score (part III)	-	17.22 ± 10.93	-
Speech (item 18)	-	1.06 ± 0.75	-
Facial expression (item 19)	-	1.22 ± 1.12	-
Resting tremor (item 20)	-	0.00 ± 0.00	-
Action or postural tremor (item 21)	-	0.22 ± 0.55	-
Rigidity (item 22)	-	3.39 ± 2.57	-
Finger tapping (item 23)	-	2.17 ± 1.34	-
Hand movement (item 24)	-	1.56 ± 1.20	-
Rapid alternating movement (item 25)	-	1.28 ± 1.27	-
Leg agility (item 26)	-	1.39 ± 1.24	-

	Healthy controls group (n = 22)	COP-induced parkinsonism Group(n = 18)	*P* value
Arising from chair (item 27)	-	0.67 ± 0.84	-
Posture (item 28)	-	0.89 ± 0.83	-
Gait (item 29)	-	1.67 ± 1.09	-
Postural stability (item 30)	-	0.89 ± 0.90	-
Body bradykinesia and hypokinesia (item31)	-	0.83 ± 0.92	-
NPI	-	13.39 ± 8.79	-

Notes: MMSE, Mini-mental state examination; MoCA, Montreal Cognitive Assessment; UPDRS III, Unified Parkinson's disease rating scale subsection III; NPI, Neuropsychiatric inventory; COP, carbon monoxide poisoning; HCs, healthy controls. *indicated $P < 0.05$.

Table 2 Clusters showing significant reduced GM volumes in patients

Brain region	Cluster size	*T* value	MNI		
			x	y	z
Olfactory_L, Caudate_L, Medial orbital SFG_L, ACC_L, Putamen_L, Amygdala_L, Putamen_R, ACC_R, Caudate_R, Medial orbital SFG_R, Amygdala_R, Olfactory_R	6512	7.74	-3	24	-4
Thalamus_L	1105	7.13	-3	-8	12
Thalamus_R	1115	7.27	3	-12	-2
MTG_L, ITG_L, Fusiform_L	1661	8.29	-57	-5	-14
MTG_R	1355	7.2	68	-42	-2
ITG_R, Fusiform_R	1900	7.1	59	-15	-30
CERCRU I_L, CERCRU VI_R	2174	6.64	-21	-71	-33
CERCRU VI_R, CERCRU I_R	1733	7.39	30	-61	-24

Notes: L, left; R, right; SFG, superior frontal gyrus; ACC, anterior cingulate cortex; MTG, middle temporal gyrus; ITG, inferior temporal gyrus; CERCRU I, crus I of cerebellum; CERCRU VI, Lobule VI of cerebellum. All cluster *P* value are corrected for false discovery rate with $P < 0.001$.

Notes: COP,carbon monoxide poisoning; SFG, superior frontal gyrus; MFG, superior frontal gyrus; SPG, superior parietal gyrus; IPG,inferior parietal gyrus; MTG, middle temporal gyrus; LOL, lateral occipital lobes. All cluster *P* value are corrected for family wise error with $P < 0.05$.

Table 3 Clusters showing significantly changed cortical morphology in the patients group

	Hemisphere	Size (vertices)	*P* value	Brain region (Overlap of atlas region, vertices size)
Patients group < Healthy controls group	Thickness			
	Left	12382	0.0000	SFG (17%, 2105)
				rostral MFG (12%, 1485)
				caudal MFG (6%, 743)
				precentral (11%, 1362)
				postcentral (12%, 743)
				SPG (10%,1238)
				IPG (5%, 619)
				LOL (7%, 867)
				precuneus (5%, 619)
	Right	6724	0.0000	SFG (27%, 1815)
				rostral MFG (20%, 1345)
				precentral (18%, 1210)
				caudal MFG (11%, 740)
		5667	0.0000	SPG (26%, 1473)
				IPG (14%, 793)
				MTG (11%, 623)
				precuneus (10%, 566)
				LOL (9%, 510)
	Sulcal depth			
	Left	242	0.0000	supramarginal (100%, 242)

Notes: COP,carbon monoxide poisoning; SFG, superior frontal gyrus; MFG, superior frontal gyrus; SPG, superior parietal gyrus; IPG,inferior parietal gyrus; MTG, middle temporal gyrus; LOL, lateral occipital lobes. All cluster *P* value are corrected for family wise error with $P < 0.05$.

Figures

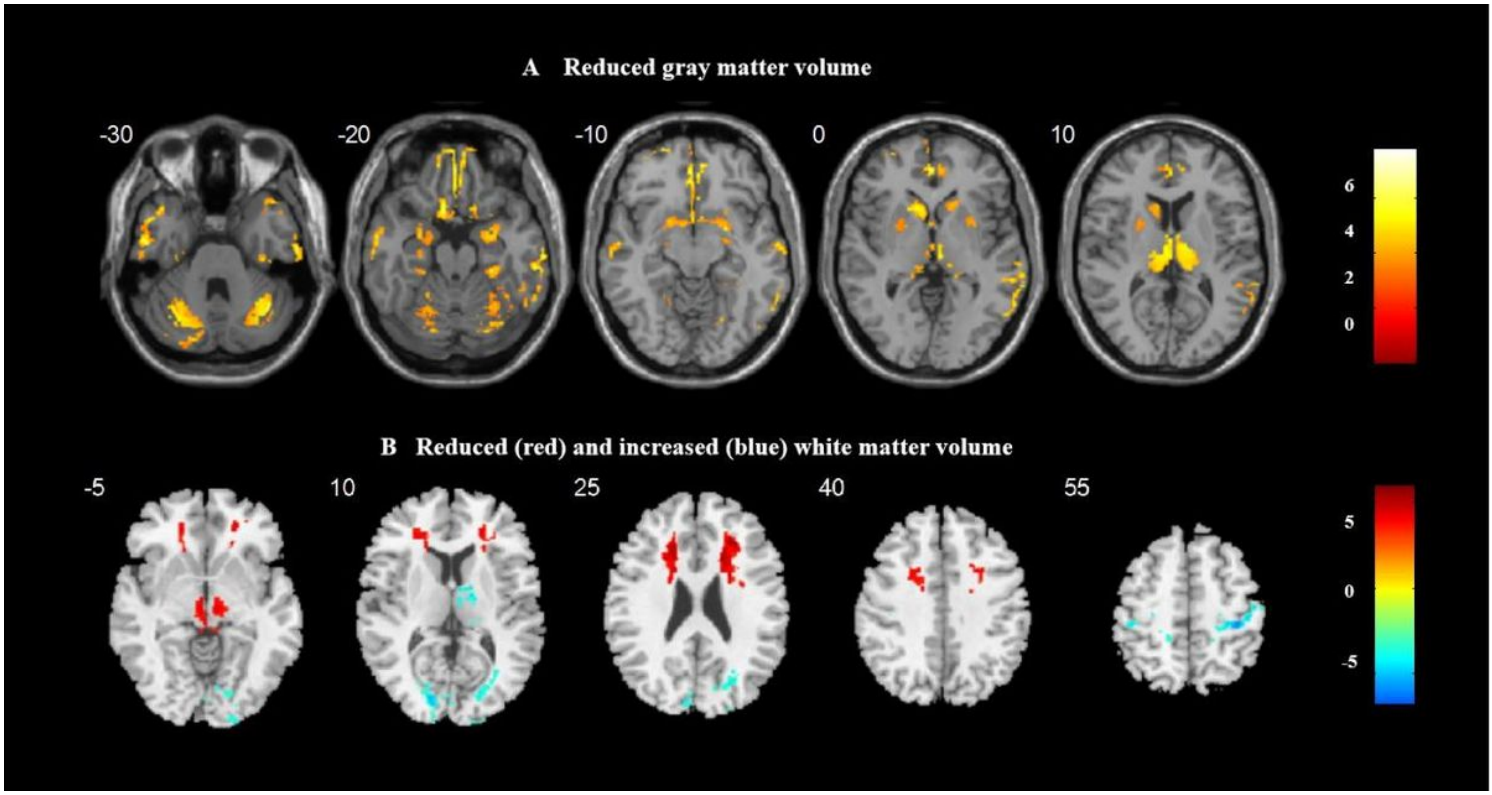

Figure 1

Volume change pattern in COP-induced parkinsonism group vs healthy controls group. A The gray matter atrophy regions in the patients group, false discovery rate corrected with a threshold at $P < 0.001$. B The white matter atrophy (red) and swelling (blue) regions in the patients group, uncorrected with a threshold at $P < 0.001$.

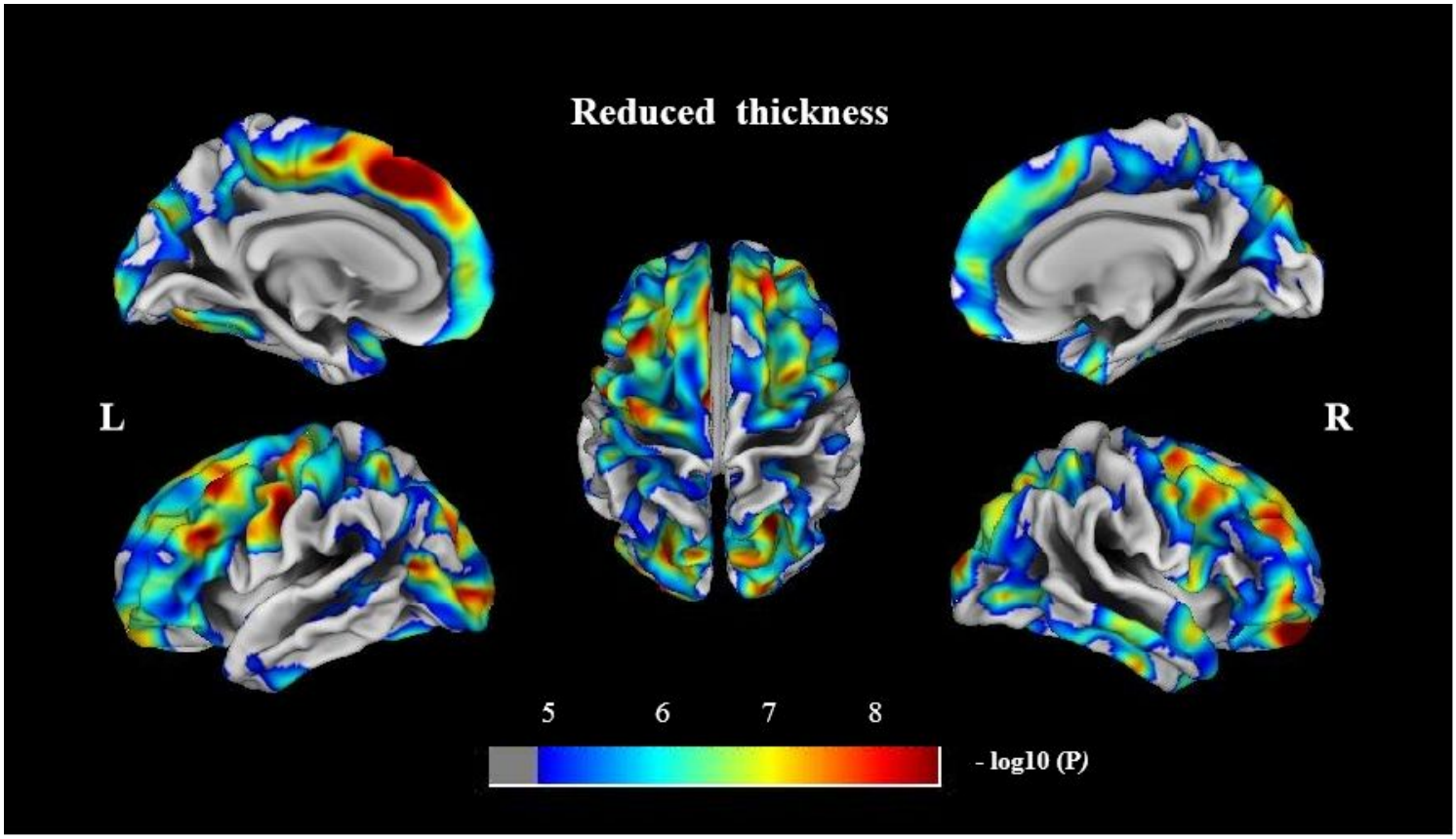

Figure 2

Widespeard cortical thinning in COP-induced parkinsonism group compared to healthy controls group. Family-wise error corrected with a threshold at $P < 0.05$.

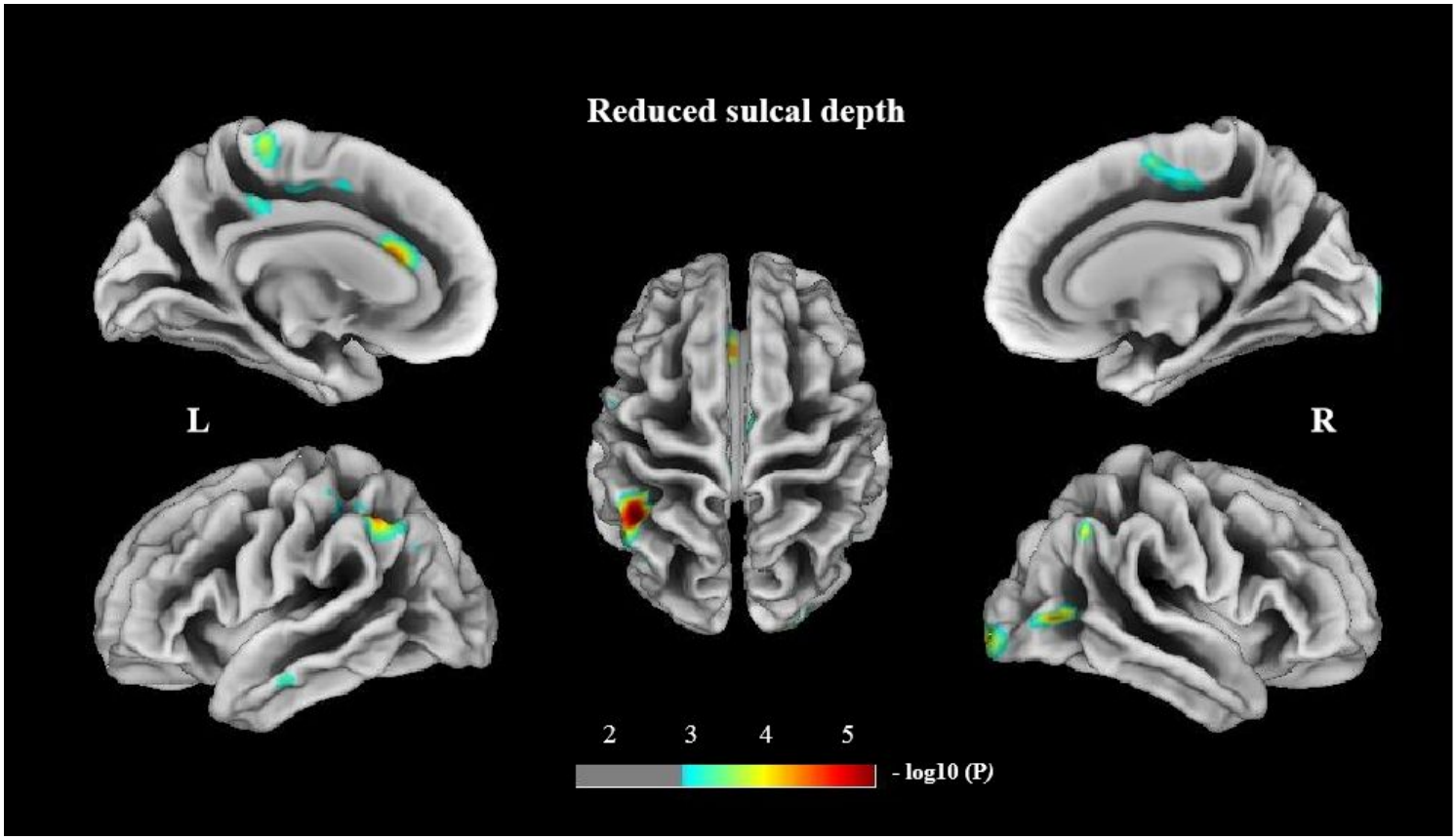

Figure 3

Shallower sulcal depth in the bilateral lateral parietal and occipital lobes, supplementary motor area, left cingulate cortex, and left middle temporal gyrus in COP-induced parkinsonism group compared to healthy controls group. Uncorrected with a threshold at $P < 0.001$.

Supplementary Files

This is a list of supplementary files associated with this preprint. Click to download.

- AuthorChecklist11682.pdf
- SupplementalTable.docx